

High T_c of liquid-quenched $\text{Bi}_{1.6}\text{Pb}_{0.4}\text{Sr}_2\text{Ga}_2\text{Cu}_3\text{O}_x$

YOSHITAKE NISHI, YUICHIRO KITA, KENJI TANIOKA

Department of Materials Science, Tokai University, Kitakaname, Hiratsuka, Kanagawa, 259-12, Japan

Although T_c cannot be found for a liquid-quenched $\text{Bi}_{1.6}\text{Pb}_{0.4}\text{Sr}_2\text{Ca}_2\text{Cu}_3\text{O}_x$ glassy sample, a high T_c is found after annealing for 24 h at 1100 K. The maximum offset temperature of the superconducting transition is 113.3 K at $2.2 \times 10^{-2} \text{ mA mm}^{-2}$. The maximum $T_{c\text{off}}$ is larger than that (the maximum $T_{c\text{off}}$ is 103.4 K at $2.0 \times 10^{-2} \text{ mA mm}^{-2}$) of sintered specimens before liquid quenching.

1. Introduction

Intensive work has been performed on high T_c Bi-Sr-Ca-Cu-O oxides [1, 2]. $T_{c\text{off}}$ of the sintered $\text{BiSrCaCu}_2\text{O}_y$ is usually below 100 K, although $T_{c\text{on}}$ is above 120 K [3]. Since the melting point of this oxide is rather low, it can be molten and liquid-quenched. The density of the liquid-quenched specimen is apparently larger than that of the sintered one, which may improve the superconducting performance of the specimen, however, $T_{c\text{off}}$ of the liquid-quenched and annealed sample is lower than that of the sintered one for $\text{BiSrCaCu}_2\text{O}_y$ [3]. Recently, it has been reported that lead addition enhances T_c (The maximum $T_{c\text{off}}$ is 111.7 K for liquid-quenched $\text{Bi}_{0.7}\text{Pb}_{0.3}\text{SrCaCu}_{1.8}\text{O}_x$ annealed for 12 h at 1120 K [4].) The effects of annealing on T_c are, therefore, investigated for the liquid-quenched $\text{Bi}_{1.6}\text{Pb}_{0.4}\text{Sr}_2\text{Ca}_2\text{Cu}_3\text{O}_x$ glassy sample.

2. Experimental procedure

Samples with nominal composition $(\text{Bi}_{1-z}\text{Pb}_z)_2\text{Sr}_2\text{Ca}_2\text{Cu}_3\text{O}_x$ were prepared by high purity powders of Bi_2O_3 (99.99%), PbO (99.99%), SrCO_3 (99.9%), CaCO_3 (99.9%) and CuO (99.9%). The powders were mixed and calcined in air at 1023 K for 6 h and then air-cooled. After crushing, the powder was sintered in air at 1073 K for 18 h and air-cooled. After crushing, pelletized tablets, 2 mm thick and 13 mm diameter, were subjected to additional sintering in air at 1123 K for 12 h and then furnace-cooled. Liquid-quenched glassy foils were prepared from chips cut from the sintered tablets using a twin-type piston-anvil apparatus shown in Fig. 1 [5-8]. The speed of the piston was about 0.12 m sec^{-1} . The structure of the samples was examined by means of X-ray diffraction. The electrical resistivity was measured using a standard four-probe technique (current density = 2 mA mm^{-2}) and a Keithley 181 nanovoltmeter. The temperature was measured by a Au*Fe-chromel thermocouple attached to the specimen in a cryostat at equilibrium temperature.

3. Results and discussion

Fig. 2 shows the temperature dependence of electrical resistivity of the $\text{Bi}_{1.6}\text{Pb}_{0.4}\text{Sr}_2\text{Ca}_2\text{Cu}_3\text{O}_x$ specimens

which are sintered before the liquid-quenching and are annealed for 24 h at 1100 K after the liquid-quenching. The electrical resistivities of the specimens show metallic decreases with temperature. Offset $T_{c\text{off}}$ and onset $T_{c\text{on}}$ of the transition are defined as the temperatures corresponding to the achievement of zero-resistivity (below $10^{-9} \Omega\text{m}$) and to the deviation of the electrical resistivity. The deviated point is taken at $dR/dT = 0.004 R_{300\text{K}}$ in the present work, where dR/dT and $R_{300\text{K}}$ are the slope of $R-T$ and the resistivity at 300 K, respectively. The midpoint of the transition is designated $T_{c\text{mid}}$. For the liquid-quenched $\text{Bi}_{1.6}\text{Pb}_{0.4}\text{Sr}_2\text{Ca}_2\text{Cu}_3\text{O}_x$ annealed for 24 h at 1100 K, $T_{c\text{off}}$, $T_{c\text{mid}}$ and $T_{c\text{on}}$ are 105.5, 114.0 and 132.9 K at 2.2 mA mm^{-2} of the current density, respectively.

Fig. 3 shows changes in $T_{c\text{off}}$, $T_{c\text{mid}}$ and $T_{c\text{on}}$ against lead substitution (z) of $(\text{Bi}_{1-z}\text{Pb}_z)_2\text{Sr}_2\text{Ca}_2\text{Cu}_3\text{O}_x$ sintered for 12 h at 1123 K. The highest T_c is found for the $\text{Bi}_{1.6}\text{Pb}_{0.4}\text{Sr}_2\text{Ca}_2\text{Cu}_3\text{O}_x$ sample which shows the modulated structure [9, 10]. The high T_c phase may show the high crystal perfection of the modulated structure. Fig. 4 shows the change in the full width at half maximum (FWHM) of X-ray diffraction against z . The lower the FWHM in Fig. 4, the higher the $T_{c\text{off}}$ in Fig. 3 becomes, that is a high degree of lattice ordering is coincident with the high $T_{c\text{off}}$.

Fig. 5 shows changes in $T_{c\text{off}}$, $T_{c\text{mid}}$ and $T_{c\text{on}}$ against the annealing temperature for the liquid-quenched $\text{Bi}_{1.6}\text{Pb}_{0.4}\text{Sr}_2\text{Ca}_2\text{Cu}_3\text{O}_x$ annealed for 1 h. Although T_c cannot be found for the liquid-quenched $\text{Bi}_{1.6}\text{Pb}_{0.4}\text{Sr}_2\text{Ca}_2\text{Cu}_3\text{O}_x$ glassy sample, the high onset temperature $T_{c\text{on}}$ above the boiling point of the liquid nitrogen

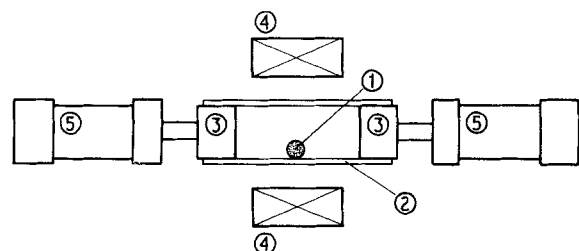


Figure 1 Schematic diagram of twin-type piston-anvil apparatus. (1 specimen, 2 quartz tube, 3 copper substrate, 4 infrared furnace, 5 air piston.)

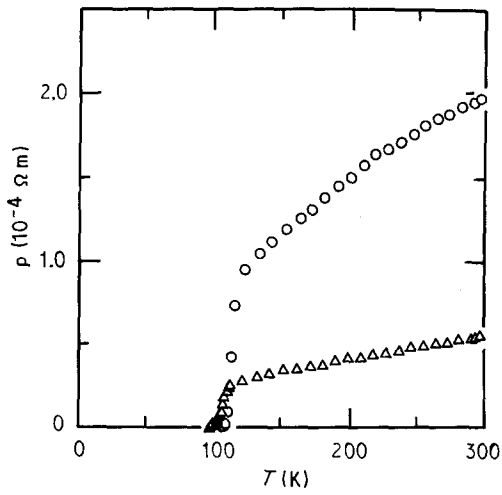


Figure 2 Change in electrical resistivity against temperature (T) for liquid-quenched and annealed (24 h \times 1100 K) $\text{Bi}_{1.6}\text{Pb}_{0.4}\text{Sr}_2\text{Ca}_2\text{Cu}_3\text{O}_x$ (O), together with a sintered sample (Δ).

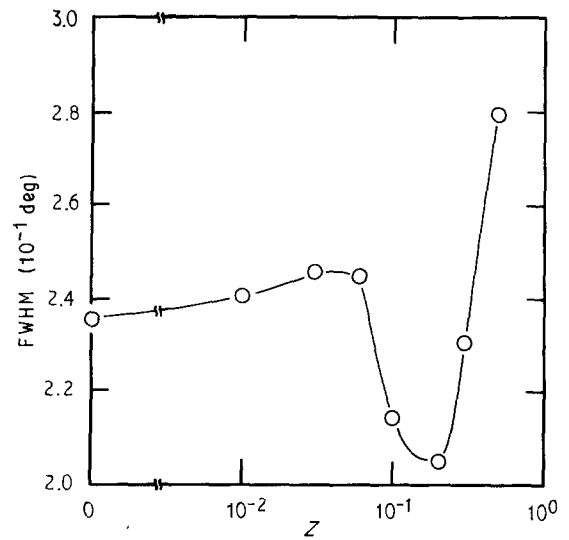


Figure 4 Values of full width at half maximum (FWHM) of X-ray diffraction peak (1170) plane against lead substitution (z) of sintered $(\text{Bi}_{1-z}\text{Pb}_z)_2\text{Sr}_2\text{Ca}_2\text{Cu}_3\text{O}_x$.

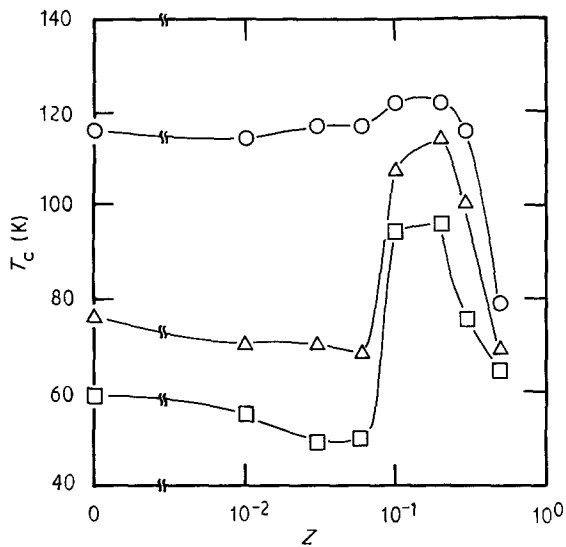


Figure 3 Change in superconducting transition temperature ($T_{c_{\text{off}}}$ (□), $T_{c_{\text{mid}}}$ (Δ) and $T_{c_{\text{on}}}$ (O)) against lead substitution (z) for sintered $(\text{Bi}_{1-z}\text{Pb}_z)_2\text{Sr}_2\text{Ca}_2\text{Cu}_3\text{O}_x$.

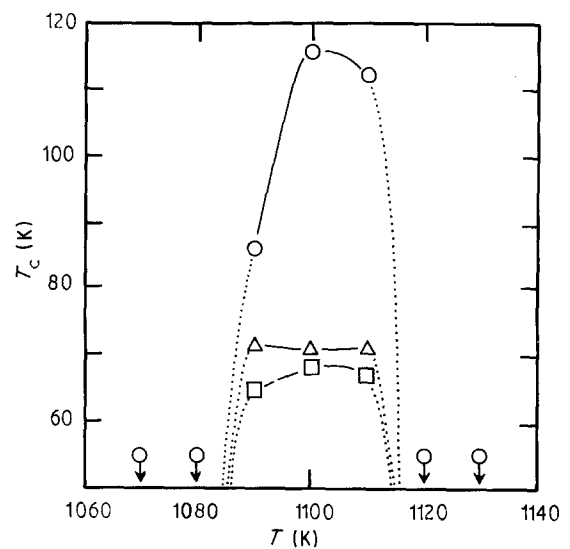


Figure 5 Change in superconducting transition temperature (T_c) against annealing temperature (T) for liquid-quenched $\text{Bi}_{1.6}\text{Pb}_{0.4}\text{Sr}_2\text{Ca}_2\text{Cu}_3\text{O}_x$ annealed for 1 h. (O on, Δ mid, □ off).

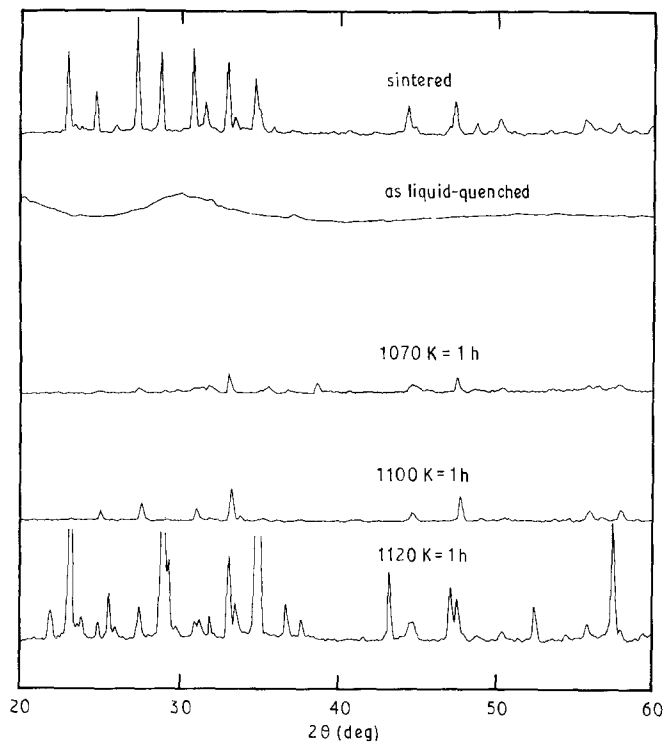


Figure 6 Diffraction pattern of liquid-quenched $\text{Bi}_{1.6}\text{Pb}_{0.4}\text{Sr}_2\text{Ca}_2\text{Cu}_3\text{O}_x$ annealed for 1 h at 1070, 1100 and 1120 K, together with sintered and as liquid-quenched glassy samples where, preset time of X-ray diffraction for glassy sample is 10 sec step.

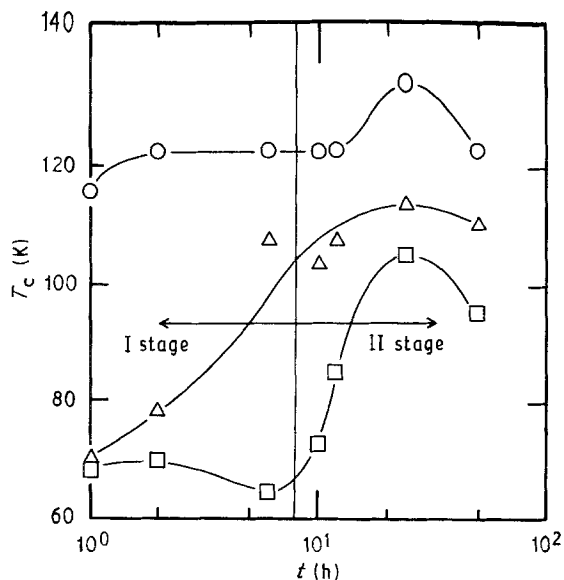


Figure 7 Change in superconducting transition temperature ($T_{c\text{off}}$ (\square), $T_{c\text{mid}}$ (Δ) and $T_{c\text{on}}$ (\circ)) against annealing time (t) for liquid-quenched $\text{Bi}_{1.6}\text{Pb}_{0.4}\text{Sr}_2\text{Ca}_2\text{Cu}_3\text{O}_x$ annealed at 1100 K. Stages I and II are for short and long periods of annealing, respectively.

is found for the crystallized sample annealed for 1 h between 1090 and 1110 K. The maximum $T_{c\text{on}}$ and $T_{c\text{off}}$ are obtained at 1100 K of the annealing temperature. The sample melted above 1120 K. The diffraction patterns of the high T_c samples annealed at 1090, 1100 and 1110 K are different from the low T_c (below 4.2 K) samples annealed at 1080 K and at 1120 K, as shown in Fig. 6.

Fig. 7 shows changes in $T_{c\text{off}}$, $T_{c\text{mid}}$ and $T_{c\text{on}}$ against annealing time for liquid-quenched $\text{Bi}_{1.6}\text{Pb}_{0.4}\text{Sr}_2\text{Ca}_2\text{Cu}_3\text{O}_x$ annealed at 1100 K. Extremely high $T_{c\text{off}}$ are

found for the crystallized samples annealing for 24 h at 1100 K. The values of the $T_{c\text{off}}$ are 105.5 K and 106.7 K, respectively.

The diffraction patterns of annealed sample in stage II is different from the annealed sample in stage I, as shown in Fig. 8. The crystallization is mainly performed for the short period of stage I. Based on the X-ray peak of the high $T_{c\text{off}}$ samples annealed in stage II, the recrystallization process formed the high T_c modulated structure [9, 10] is probably performed.

Fig. 9 shows changes in the lattice constant (c) of the c axis against the annealing time at 1100 K. The higher the lattice constant during stage II in Fig. 9, the higher the $T_{c\text{off}}$ in Fig. 7 becomes. The high T_c phase is explained by the formation of the copper-concentrated bands in the modulated structure for the Bi-Sr-Ca-Cu-O [9-11]. The number of the copper-concentrated bands in the perovskite layer agrees with the c axis value for Tl-Ba-Ca-Cu-O [12-14]. Figs 7 and 9 show that the extremely high T_c sample is constructed by the modulated structure which shows maximum T_c . An excess period of the annealing decreases the lattice constant. The transition of the modulated structure mainly decreases T_c .

Fig. 10 shows changes in the full width at half maximum (FWHM) against the annealing time at 1100 K. The lower the FWHM of stage II in Fig. 10, the higher the $T_{c\text{off}}$ in Fig. 7 becomes. Figs 7 and 10 show that the extremely high T_c sample shows the extremely high crystal perfection of the modulated structure. An excess period of the annealing increases FWHM. The transition of the modulated structure induces disordering and then decreases T_c .

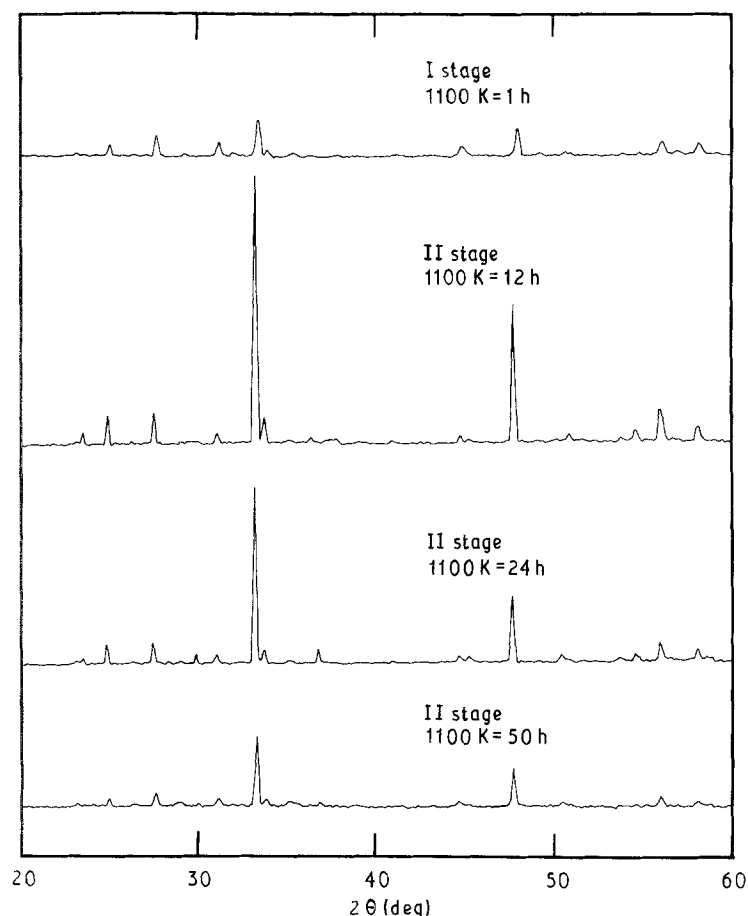


Figure 8 Diffraction pattern of liquid-quenched $\text{Bi}_{1.6}\text{Pb}_{0.4}\text{Sr}_2\text{Ca}_2\text{Cu}_3\text{O}_x$ annealed at 1100 K. Stages I and II are for short and long periods of annealing, respectively.

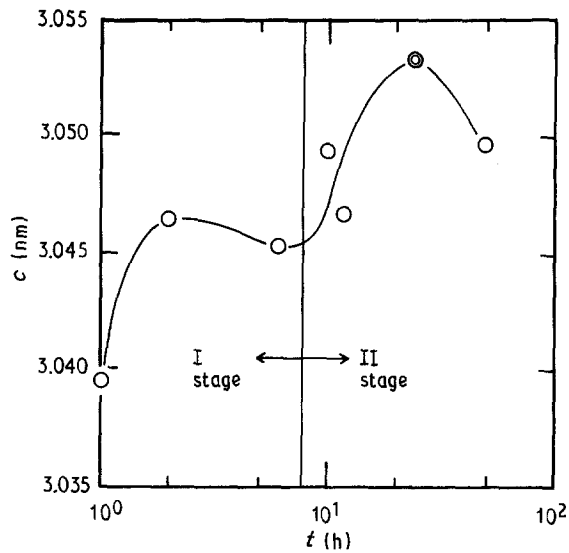


Figure 9 Change in lattice constant (c axis) against annealing time (t) of liquid-quenched $\text{Bi}_{1.6}\text{Pb}_{0.4}\text{Sr}_2\text{Ca}_2\text{Cu}_3\text{O}_x$ annealed at 1100 K. Stages I and II are for short and long periods of annealing, respectively. Both values for liquid-quenched $\text{Bi}_{1.6}\text{Pb}_{0.4}\text{Sr}_2\text{Ca}_2\text{Cu}_3\text{O}_x$ samples annealed for 24 h at 1100 K show mark (⊙).

$T_{\text{c off}}$ depends on the current density. Fig. 11 shows $T_{\text{c off}}$ change against I for the $\text{Bi}_{1.6}\text{Pb}_{0.4}\text{Sr}_2\text{Ca}_2\text{Cu}_3\text{O}_x$ samples annealed for 24 h at 1100 K, together with the sintered sample before liquid quenching. $T_{\text{c off}}$ increases with I decreasing. The detectable maximum $T_{\text{c off}}$ is 113.3 K at $2.2 \times 10^{-2} \text{ mA mm}^{-2}$ for one of the liquid-quenched and annealed $\text{Bi}_{1.6}\text{Pb}_{0.4}\text{Sr}_2\text{Ca}_2\text{Cu}_3\text{O}_x$ samples. The temperature is larger than that ($T_{\text{c off}} = 103.4 \text{ K}$ at $2.0 \times 10^{-2} \text{ mA mm}^{-2}$) of the sintered $\text{Bi}_{1.6}\text{Pb}_{0.4}\text{Sr}_2\text{Ca}_2\text{Cu}_3\text{O}_x$.

4. Conclusion

The affects of annealing on T_c are investigated. Although T_c cannot be found for liquid-quenched $\text{Bi}_{1.6}\text{Pb}_{0.4}\text{Sr}_2\text{Ca}_2\text{Cu}_3\text{O}_x$ glassy sample, an extremely high T_c is

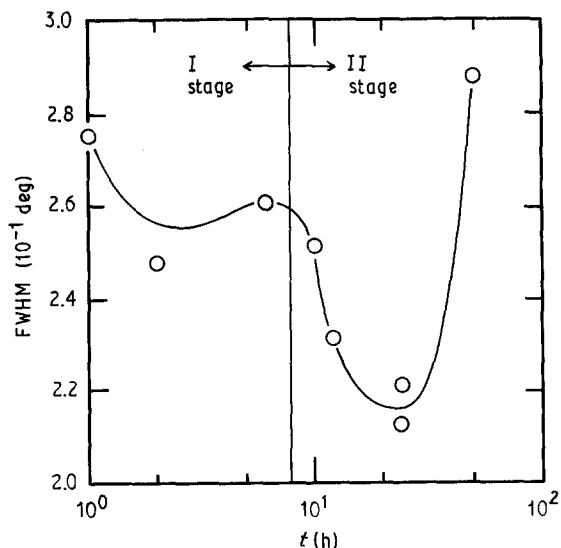


Figure 10 Value of full width at half maximum of X-ray diffraction peak of (1170) plane of liquid-quenched $\text{Bi}_{1.6}\text{Pb}_{0.4}\text{Sr}_2\text{Ca}_2\text{Cu}_3\text{O}_x$ annealed at 1100 K. Stages I and II are for short and long periods of annealing, respectively.

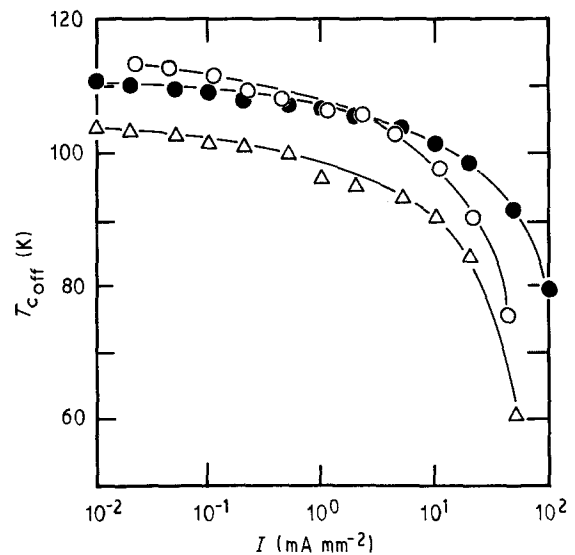


Figure 11 Change in offset temperature ($T_{\text{c off}}$) against current density (I) for liquid-quenched $\text{Bi}_{1.6}\text{Pb}_{0.4}\text{Sr}_2\text{Ca}_2\text{Cu}_3\text{O}_x$ samples (O, ●) annealed for 24 h at 1100 K, together with a sintered sample (Δ).

found after annealing for 24 h at 1100 K. The detectable maximum $T_{\text{c off}}$ is 113.3 K at $2.2 \times 10^{-2} \text{ mA mm}^{-2}$. The maximum $T_{\text{c off}}$ is larger than that (the maximum $T_{\text{c off}}$ is 103.4 K) of the sintered specimen.

References

1. H. MAEDA, Y. TANAKA, M. FUKUTOMI and T. ASANO, *Jpn J. Appl. Phys.* **27** (1988) L209.
2. H. MAEDA, Y. TANAKA, M. FUKUTOMI, T. ASANO, K. TOGANO, H. KUMAKURA, M. UEHARA, S. IKEDA, K. OGAWA, S. HORIUCHI and Y. MATSUI, *Physica C* **155** (1988) 602.
3. Y. NISHI, S. MORIYA, S. TOKUNAGA and K. TACHIKAWA, *J. Mater. Sci. Lett.* **8** (1989) 247.
4. Y. NISHI, S. MORIYA and T. MANABE, *J. Appl. Phys.* **65** (1989) 2389.
5. Y. NISHI, M. KAWAKAMI and K. MIKAGI, *J. Mater. Sci.* **32** (1987) 554.
6. Y. NISHI, T. KAI and K. KITAGO, *Wear* **126** (1988) 191.
7. Y. NISHI and H. HARANO, *J. Appl. Phys.* **63** (1988) 1141.
8. Y. NISHI, H. HARANO, T. FUKUNAGA and K. SUZUKI, *Phys. Rev. B* **37** (1988) 2855.
9. E. TAKAYAMA-MUROMACHI, Y. UCHIDA, Y. MATSUI, M. ONODA and K. KATO, *Jpn J. Appl. Phys.* **27** (1988) 556.
10. A. ONO, K. KOSUDA, S. SUENO and Y. ISHIZAWA, *ibid.* **27** (1988) 1077.
11. Y. HIROTSU, O. TOMIOKA, T. OHKUBO, N. YAMAMOTO, Y. NAKAMURA, S. NAGAKURA, T. KOMATSU and K. MATSUSHITA, *ibid.* **27** (1988) 1869.
12. Y. SYONO and M. KIKUCHI, *Bull. Jpn Inst. Met.* **27** (1989) 574.
13. S. IJIMA, T. ICHIHASHI and Y. KUBO, *Jpn J. Appl. Phys.* **27** (1988) L817.
14. M. A. SUBRAMANIAN, J. C. CALABRESE, C. C. TORARDI, J. GAPALAKRISHNAN, T. R. ASKEW, R. B. FLIPPEN, K. J. MORRISEY, U. CHOWDHRY and A. W. SLEIGHT, *Nature* **332** (1988) 420.

Received 20 July
and accepted 22 November 1989